

# Reaction Rate of Olive Stone during Combustion in a Bubbling Fluidized Bed

A. Soria-Verdugo, M. Rubio-Rubio, J. Arrieta, N. García-Hernando

**Abstract**—Combustion of biomass is a promising alternative to reduce the high pollutant emission levels associated to the combustion of fossil fuels due to the net null emission of CO<sub>2</sub> attributed to biomass. However, the biomass selected should also have low contents of nitrogen and sulfur to limit the NO<sub>x</sub> and SO<sub>x</sub> emissions derived from its combustion. In this sense, olive stone is an excellent fuel to power combustion reactors with reduced levels of pollutant emissions. In this work, the combustion of olive stone particles is analyzed experimentally in a thermogravimetric analyzer (TGA) and in a bubbling fluidized bed reactor (BFB). The bubbling fluidized bed reactor was installed over a scale, conforming a macro-TGA. In both equipment, the evolution of the mass of the samples was registered as the combustion process progressed. The results show a much faster combustion process in the bubbling fluidized bed reactor compared to the thermogravimetric analyzer measurements, due to the higher heat transfer coefficient and the abrasion of the fuel particles by the bed material in the BFB reactor.

**Keywords**—Olive stone, combustion, reaction rate, thermogravimetric analysis, fluidized bed.

## I. INTRODUCTION

DUE to environmental reasons derived from the current high pollutant emission levels, there is a requirement of looking for alternatives to fossil fuels on which heating applications can be based. In this regard, solid fuels derived from biomass are a promising alternative to fossil fuels in small-scale heating applications, such as residential heating systems. These biomass systems substitute conventional fossil-fuel-based furnaces by biomass-powered units. Biomass furnaces are designed to operate with a broad range of biomass types, provided that the particle size is in a narrow range and its density is high enough. These requirements of controlled size and high density of the particles involve additional energy input for splintering and pelleting for most lignocellulosic residual biomasses. In contrast to other biomass types, olive stones are a high energetic dense residual biomass with an adequate particle size for biomass furnaces, without the need of pelletizing, thus, avoiding the additional energy consumption in fuel pre-processing. In comparison to other biomass sources, characterized by high contents of sulfur and nitrogen [1], the contents of these components in olive stones are low, which minimizes the emission of nitrogen oxides and sulfur oxides during its combustion [2]. Also, olive stones are characterized by low contents of chlorine, sodium, and potassium, which

diminish the risk of corrosion and soiling of the furnace [3].

The production of olive stones as a residue of the olive industry in the south of Europe is enormous, especially in Spain, Italy, and Portugal. In Andalusia (south of Spain) alone, the average annual production of olive stones is around 360,000 tons [4]. These olive stones can be used directly as a solid fuel, or they can be subjected to drying or torrefaction processes before its use to increase their heating value [5].

Combustion of solid fuels is a complex process which involves drying and pyrolysis inside the solid fuel particle, and combustion of both the pyrolysis vapors produced and the char formed at the surface of the particle. Accurately modeling of solid fuels combustion is still a challenge, which can serve as a useful tool to improve the design of residential and industrial solid fuel burners. There are several models of biomass combustion available in the literature, with different levels of detail and complexity [6]-[10]. These models require validation with experimental measurements; however, the availability of accurate and reliable experimental results concerning combustion of olive stones in the literature is scarce.

Fluidized beds are employed as industrial chemical reactors because of their ability to convert solid fuels with a high efficiency. These systems are characterized by high heat transfer coefficients, great surface area available for heat transfer or chemical reaction, and proper mixing of fuel particles and bed material. Due to these advantages, fluidized bed reactors are widely used to hold combustion reactions of solid fuels. The homogeneous and moderate temperature in fluidized beds limits emissions of NO<sub>x</sub> as a product of the combustion process. At the same time, sorbent bed materials can be used for in-bed capture of SO<sub>x</sub> emissions. Therefore, fluidized beds are an excellent alternative to build combustors powered by solid fuels.

In this paper, the combustion of olive stone particles is studied experimentally in both a thermogravimetric analyzer (TGA) and in a lab-scale bubbling fluidized bed (BFB). The non-isothermal combustion in the TGA is analyzed for various heating rates of the particles, whereas in the BFB, the combustion occurs at a constant temperature of 600°C. In both cases, the time evolution of the mass remaining in the reactor is monitored as the combustion process progresses, reporting these relevant experimental measurements to validate mathematical models of solid fuels combustion.

A. Soria-Verdugo is with the University Carlos III, Department of Thermal Engineering and Fluid Mechanics. Avda. de la Universidad 30, 28911, Leganés, Madrid, Spain (phone: +34 91 624 8465; e-mail: asoria@ing.uc3m.es).

M. Rubio-Rubio is with the University of Jaen, Department of Mechanical and Mining Engineering, Spain (e-mail: mrubio@ujaen.es).

J. Arrieta Mediterranean is with the Institute for Advanced Studies, Spain (UIB-CSIC) (e-mail: jarrieta@imedea.uib-csic.es).

N. Garcia-Hernando is with the University Carlos III, Department of Thermal Engineering and Fluid Mechanics, Spain (e-mail: ngarcia@ing.uc3m.es).

## II. MATERIALS AND METHODS

### A. Biomass Characterization

Olive stone, with a particle size around 500  $\mu\text{m}$ , was used for the combustion tests, both in the TGA and in the lab-scale bubbling fluidized bed. A basic characterization of the biomass samples, consisting in a proximate and an ultimate analysis, was performed prior to the combustion experiments.

The proximate analysis was conducted in a TGA Q500 from TA Instruments. The moisture content was determined as the percentage of mass released by the sample during an isothermal process at 105°C in an inert atmosphere, and the volatile matter was measured as the percentage of mass released when subjecting the sample to a heating process up to 900°C, also in an inert atmosphere. The inert atmosphere required to measure the moisture and volatile matter contents was guaranteed supplying the TGA furnace with a flowrate of 60 ml/min of nitrogen. In contrast, the ash content was determined as the mass percentage remaining after a combustion process at 550°C, supplying the TGA furnace with a flowrate of 60 ml/min of oxygen. Once the moisture, volatile matter, and ash contents of the samples were obtained, the fixed carbon content was determined by difference.

The ultimate analysis of the olive stone samples was conducted in LECO TruSpec CHN and TruSpec S analyzers. Carbon, hydrogen and sulfur contents of the samples were determined measured by means of infrared absorption detectors for the exhaust gases obtained after a complete combustion of the olive stones in an atmosphere of pure oxygen. However, the nitrogen content was determined conducting the exhaust gases through a thermal conductivity cell.

TABLE I  
 RESULTS OBTAINED FROM THE PROXIMATE AND ULTIMATE ANALYSIS OF THE OLIVE STONE SAMPLES

Proximate Analysis	
Volatile matter [%d]	77.0
Fixed carbon* [%d]	22.3
Ash [%d]	0.7
Ultimate Analysis	
C [%daf]	52.4
H [%daf]	6.1
N [%daf]	0.9
S [%daf]	0.1
O* [%daf]	40.5

d: dry basis, daf: dry-as-free basis, \* obtained by difference

The results of both the proximate and ultimate analyses of the olive stone samples used in the combustion tests are reported in Table I. The high volatile matter content and, principally, the low ash content of olive stones are very favorable characteristics for solid fuel combustion applications, which position olive stones as an attractive renewable energy source. This low ash content reduced the requirement of ash removal from the furnace and the risk of damage to the equipment due to corrosion caused by the ash fusibility in high temperature combustion applications. The contents of nitrogen and sulfur of olive stones are low in comparison with typical

values found in biomass, which is crucial for clean combustion applications, considering that these contents end as nitrogen oxides and sulfur oxides pollutant emissions. Further details of the proximate and ultimate analyses can be found elsewhere [11]-[13].

### B. Thermogravimetric Analyzer

The thermogravimetric analyzer employed for the combustion tests of olive stones is the same TGA apparatus. The precision of the equipment for the measurement of mass and temperature is  $\pm 0.01\%$  and  $\pm 0.1^\circ\text{C}$ , respectively.

A flowrate of 60 ml/min of oxygen was supplied to the furnace to generate and oxidant atmosphere. The mass of the sample of olive stones was 80 mg for all the tests. The temperature profile during the combustion tests consisted in a linear increase from room temperature to the desired maximum temperature at a constant heating rate, followed by an isothermal process for 10 min. The maximum temperature was selected as 600°C and five different values of the heating rate 25°C/min, 50°C/min, 75°C/min, 100°C/min and the maximum possible, using the function “jump” of the TGA, were tested. Besides, each combustion test was replicated to check the repetitiveness and reliability of the measurement. Therefore, a total of 10 different combustion experiments were conducted in the thermogravimetric analyzer.

### C. Lab-Scale Bubbling Fluidized Bed

Combustion tests of olive stones were also conducted in a lab-scale bubbling fluidized bed reactor. The reactor vessel was cylindrical, with an internal diameter of 4.7 cm and a height from the distributor of 50 cm. The reactor wall, made of stainless steel, was surrounded by four electric resistors capable of supplying a total thermal power of 2 kW to increase and maintain the temperature of the reactor. A potentiometer controlled the thermal power released by the resistors, enabling the control of the temperature inside the reactor. Air was employed as fluidizing agent, and the flowrate was measured by a SMC flow meter. The reactor was installed over a high precision scale PS 6000 R2 from RADWAG with a mass precision of 0.01 g. The scale measured the mass released by the olive stone particles during their combustion inside the sample. A schematic illustration of the experimental facility is depicted in Fig. 1. This system has already been used to study the pyrolysis process of sewage sludge [14] and *Cynara cardunculus* L. [15] particles immersed in a bubbling fluidized bed reactor.

The combustion test in the lab-scale reactor consisted in heating the bed up to 600°C while fluidizing with air. Once the bed was at the desired temperature, the gas velocity was adjusted to double the minimum fluidization velocity, corresponding to a bubbling fluidized bed regime. Then, the sample of 10 g of olive stone particles was supplied through the top of the bed as a batch, and the mass measurement of the scale was registered as the combustion process progressed, while the olive stone particles move freely inside the bed.

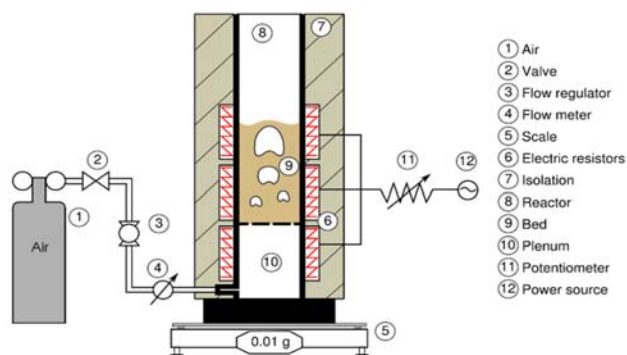


Fig. 1 Schematic of the lab-scale bubbling fluidized bed reactor.

#### D. Bed Material Characterization

The bed material employed during the combustion tests in the lab-scale bubbling fluidized bed was silica sand, which are known to be inert particles during the combustion process. The particle size of the silica sand was in the range of 425 – 600  $\mu\text{m}$ , and their particle density was,  $\rho_{\text{bm}}$ , 2600  $\text{kg}/\text{m}^3$ . The fixed bed height was selected as 9.4 cm for all the combustion tests, corresponding to a bed aspect ratio of 2. The mass of silica sand required to reach the desired height is 240 g, resulting in a void fraction,  $\varepsilon$ , of 0.44.

The minimum fluidization velocity,  $U_{\text{mf}}$ , of the silica sand particles employed was measured as a function of the bed temperature,  $T$ , by visual inspection, as the gas velocity for which bubbles start to appear on the bed surface, since these silica sand particles correspond to type B particles according to the classification of Geldart [16]. These type B particles are characterized by coincident values for the minimum fluidization and minimum bubbling velocities [17]. The evolution of the minimum fluidization velocity with temperature can also be estimated using the correlation of Carman-Kozeny (CK) [18]:

$$U_{mf} = \frac{(\phi d_{bm})^2 (\rho_{bm} - \rho_g) g \varepsilon^3}{180 \mu_g (1 - \varepsilon)}, \quad (1)$$

being  $U_{\text{mf}}$  the minimum fluidization velocity of the silica sand particles,  $\phi$  their sphericity,  $\varepsilon$  the void fraction of the dense phase,  $g$  the gravity acceleration,  $d_{\text{bm}}$  the average diameter of the particles,  $\rho_{\text{bm}}$  their density, and  $\rho_g$  and  $\mu_g$  the density and dynamic viscosity of the fluidizing air at the bed temperature, respectively.

Considering air as an ideal gas, the variation of the density,  $\rho_g$ , and viscosity,  $\mu_g$ , with temperature can be estimated as described in Sánchez-Prieto et al. [19]. The density of air was calculated as follows:

$$\rho_g = \rho_{g,amb} \frac{T_{amb}}{T}, \quad (2)$$

where  $T$  is the bed temperature,  $\rho_g$  is the air density, and  $\rho_{g,amb}$  is the air density at the reference temperature,  $T_{\text{amb}} = 300 \text{ K}$ .

The value of the air density at the reference temperature is  $\rho_{g,amb} = 1.16 \text{ kg}/\text{m}^3$ .

The dynamic viscosity of air can be calculated as a function of temperature,  $T$ , by the following potential law:

$$\mu_g = \mu_{g,amb} \left( \frac{T}{T_{amb}} \right)^{2/3}, \quad (3)$$

considering the dynamic viscosity of air at the reference temperature,  $T_{\text{amb}} = 300 \text{ K}$ , as  $\mu_{g,amb} = 1.85 \cdot 10^{-5} \text{ kg}/(\text{m}\cdot\text{s})$ .

The measured values of the minimum fluidization velocity,  $U_{\text{mf}}$ , of silica sand are plotted in Fig. 2 as a function of the bed temperature,  $T$ . The evolution of the minimum fluidization velocity with temperature predicted by the Carman-Kozeny correlation, (1), is also represented in Fig. 2, considering an average bed material diameter of  $d_{\text{bm}} = 512.5 \mu\text{m}$  and a sphericity of  $\phi = 0.8$  for the silica sand particles. A very good agreement between the estimation of the Carman-Kozeny correlation and the experimental measurements can be observed in Fig. 2.

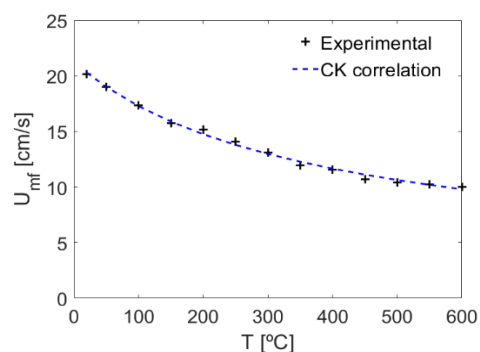


Fig. 2 Evolution of the minimum fluidization velocity with the bed temperature

### III. RESULTS AND DISCUSSION

#### A. Combustion Tests in the TGA

During the combustion of the olive stone samples in the thermogravimetric analyzer, the time evolution of the mass of the sample was registered for each temperature profile, i.e., for the various heating rates analyzed. From the mass of the sample,  $m$ , the percentage of mass remaining,  $X$ , can be calculated considering the initial mass of olive stones at the beginning of the tests,  $m_0$ . As an example, the time evolution of the mass percentage remaining and its time derivative can be observed in Fig. 3 for a heating rate of 50°C/min. The complexity of the combustion of solid fuels can be confirmed in view of Fig. 3.

The combustion process of solid fuels is composed of several processes occurring either sequentially or simultaneously. First, as the temperature of the solid fuel particle increases, drying occurs. In the case of Fig. 3, the drying process occurs during the first 5 min of the test, when the temperature increases from room temperature up to around 250°C. For higher temperatures,

the release and combustion of volatile matter arises, which is observed in Fig. 3 as a sudden decrease of the mass percentage remaining for the X-t curve and as various steep peaks, which might be attributed to different volatile species, in the dX/dt-t curve. Then, once the release of volatile matter ends, combustion of char, which is a much slower process, happens.

The char combustion is detected as a roughly constant value of the ratio of change of the percentage of mass, dX/dt, and lower than that corresponding to the release of volatiles matter. Finally, the ash content of the sample remains as a mineral residue at the end of the combustion process.

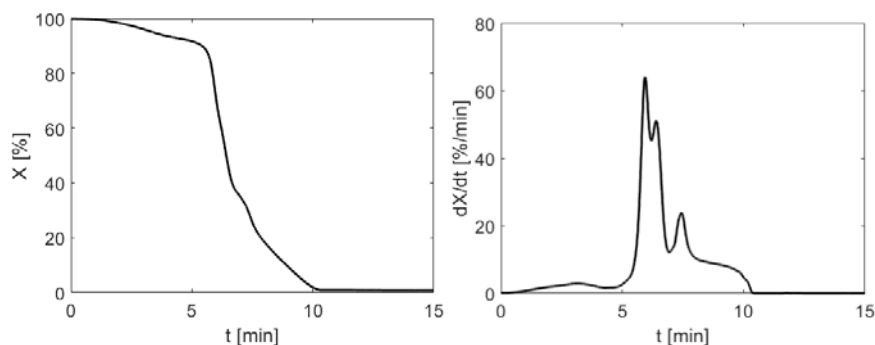


Fig. 3 Time evolution of the percentage of mass (left) and its time derivative (right) during the combustion test in the TGA for a heating rate of 50 °C/min

The degree of conversion,  $\alpha$ , can be calculated from the percentage of mass remaining as follows:

$$\alpha = 100 \frac{100 - X}{100 - X_{end}}, \quad (4)$$

where X is the percentage of mass remaining at time t and  $X_{end}$  is the percentage of mass remaining at the end of the combustion process, i.e., the ash content of the sample.

The degree of conversion determined using (4) is 0% at the beginning of the combustion process and 100% once the combustion process ends. The time evolution of the degree of conversion during the combustion process of olive stones in the thermogravimetric analyzer for the various heating rates tested is shown in Fig. 4. The combustion process is accelerated for higher heating rates. The drying and volatile matter released occur sequentially for low heating rates, e.g.,  $\beta = 25^\circ\text{C}/\text{min}$ , however, for faster heating rates, e.g., the “jump” case, the rapid heating of the particle lead to the almost simultaneous release of moisture and volatile matter. In contrast, the combustion of char is a much slower process than drying and devolatilization, and thus, this sub-process is controlled by the chemical kinetics instead of the heat transfer. This can be observed in Fig. 4, where the slope in the degree of conversion for higher values than 80%, i.e., once the volatile matter is released and only char remains in the pan, is the same for all cases.

#### B. Combustion Tests in the Bubbling Fluidized Bed Reactor

The results obtained from the combustion experiments in the lab-scale reactor are similar to those attained in the thermogravimetric analyzer. In fact, the lab-scale reactor can be considered as a macro-TGA, where also the fluid dynamics of the reactor can be accounted for.

The percentage of mass remaining in the bed when operating under a bubbling fluidized regime is shown in Fig. 5. In this figure, the fast combustion process of the olive stone particles

due to the high heat transfer coefficients associated to fluidized beds can be confirmed. A vibration can also be observed in the mass signal registered by the scale, as a result of the ascending motion of gas bubbles inside the bed. In contrast to the results of the combustion process in the TGA, the heating process of the olive stone particles in the bubbling fluidized bed is so fast that the different sub-processes, i.e., drying, volatile matter release, and char combustion, cannot be distinguished.

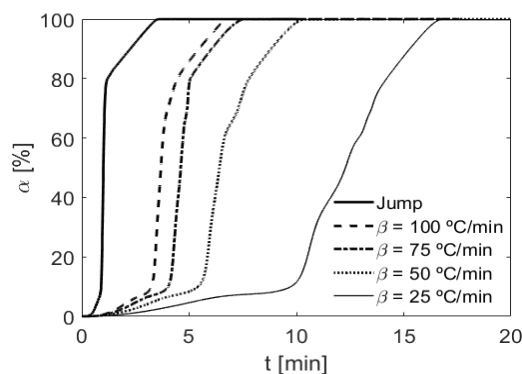


Fig. 4 Time evolution of the degree of conversion during the combustion of olive stones in a TGA for various heating rates,  $\beta$

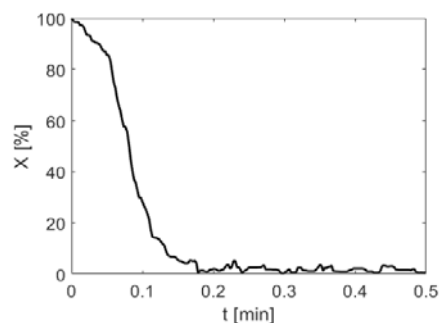


Fig. 5 Percentage of mass remaining in the bed for the combustion of olive stone particles in a bubbling fluidized bed

The degree of conversion during the combustion of olive stones in the bubbling fluidized bed can also be calculated with (4), considering the percentage of mass remaining in the bed shown in Fig. 5. The time evolution of the degree of conversion during the combustion in the bubbling fluidized bed is represented in Fig. 6.

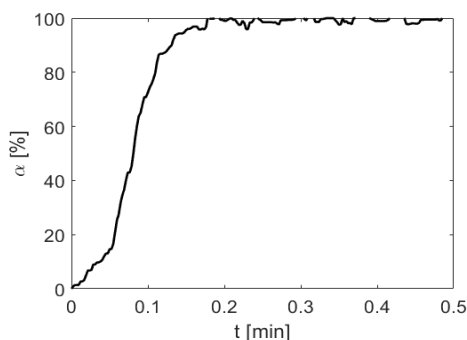


Fig. 6 Degree of conversion for the combustion of olive stone particles in a bubbling fluidized bed

Compared to the results of the combustion tests in the TGA, depicted in Fig. 4, the process is significantly accelerated in the bubbling fluidized bed. In fact, even the slow combustion of char occurs faster in the fluidized bed. This is caused by the char generated by the abrasion of the silica sand particles conforming the bed, increasing the contact surface of char and oxygen, which promotes the faster combustion of char. Therefore, the reaction rate of olive stone combustion is much higher in a bubbling fluidized bed reactor than in a thermogravimetric analyzer.

#### IV. CONCLUSIONS

The combustion process of olive stone particles was studied in a thermogravimetric analyzer and in a lab-scale bubbling fluidized bed. The non-isothermal combustion process in the TGA was affected by the heating rate employed. For low heating rates, drying, release of volatile matter and char combustion occur sequentially. Drying and volatile matter release is controlled by heat transfer, whereas char combustion, which is much slower, is controlled by the chemical kinetics. The results obtained for the combustion of olive stone in the bubbling fluidized bed reactor show an acceleration of the process in this system due to the high heat transfer coefficients associated to fluidized beds, which promotes a fast heating of the olive stone particles. Even the slow combustion of char is accelerated in the bubbling fluidized bed as a result of the abrasion of char caused by the motion of the bed material. As a general conclusion, the reaction rate during the combustion of olive stone particles is higher in a bubbling fluidized bed reactor.

#### REFERENCES

[1] M. Hupa, O. Karlström, E. Vainio, "Biomass combustion technology development – It is all about chemical details", *Proceedings of the Combustion Institute* vol. 36 pp. 113-134, 2017.  
[2] J. F. González, C. M. González-García, A. Ramiro, J. González, E. Sabio, J. Gañán, M. A. Rodríguez, "Combustion optimisation of biomass residue

pellets for domestic heating with a mural boiler", *Biomass & Bioenergy* vol. 27 pp. 145-154, 2004.  
[3] T. Miranda, A. Esteban, S. Rojas, I. Montero, A. Ruiz, "Combustion Analysis of Different Olive Residues", *International Journal of Molecular Sciences* vol. 9 pp. 512-525, 2008.  
[4] F. J. Gómez-de la Cruz, P. J. Casanova-Peláez, J. M. Palomar-Carnicero, F. Cruz-Peragón, "Drying kinetics of olive stone: A valuable source of biomass obtained in the olive oil extraction", *Energy* vol. 75 pp. 146-152, 2014.  
[5] F. F. Costa, G. Wang, M. Costa, "Combustion kinetics and particle fragmentation of raw and torrefied pine shells and olive stones in a drop tube furnace", *Proceedings of the Combustion Institute* vol. 35 pp. 3591-3599, 2015.  
[6] H. Thunman, B. Leckner, F. Niklasson, F. Johnsson, "Combustion of wood particles – A particle model for Eulerian calculations", *Combustion and Flame* vol. 129 pp. 30-46, 2002.  
[7] Y. Haseli, J.A. van Oijen, L.P.H. de Goeij, "A detailed one-dimensional model of combustion of a woody biomass particle", *Bioresource Technology* vol. 102 pp. 9772-9782, 2011.  
[8] X. Jiang, D. Chen, Z. Ma, J. Yan, "Models for the combustion of single solid fuel particles in fluidized beds: A review", *Renewable and Sustainable Energy Reviews* vol. 68 pp. 410-431, 2017.  
[9] J. Porteiro, J. L. Míguez, E. Granada, J.C. Moran, "Mathematical modelling of the combustion of a single wood particle", *Fuel Processing Technology* vol. 87 pp. 169-175, 2006.  
[10] J. Porteiro, E. Granada, J. Collazo, D. Patiño, J.C. Morán, "A model for the combustion of large particles of densified wood", *Energy & Fuels* vol. 21 pp. 3151-3159, 2007.  
[11] A. Soria-Verdugo, E. Goos, J. Arrieta-Sanagustín, N. Garcia-Hernando, "Modeling of the pyrolysis of biomass under parabolic and exponential temperature increases using the Distributed Activation Energy Model", *Energy Conversion and Management* vol. 118 pp. 223-230, 2016.  
[12] A. Soria-Verdugo, E. Goos, N. Garcia-Hernando, U. Riedel, "Analyzing the pyrolysis kinetics of several microalgae species by various differential and integral isoconversional kinetic methods and the Distributed Activation Energy Model", *Energy Conversion and Management* vol. 32 pp. 11-29, 2018.  
[13] A. Soria-Verdugo, M. Rubio-Rubio, E. Goos, U. Riedel, "Combining the Lumped Capacitance Method and the simplified Distributed Activation Energy Model to describe the pyrolysis of thermally small biomass particles", *Energy Conversion and Management* vol. 175 pp. 164-172, 2018.  
[14] A. Soria-Verdugo, A. Morato-Godino, L. M. García-Gutiérrez, N. García-Hernando, "Pyrolysis of sewage sludge in a fixed and a bubbling fluidized bed – Estimation and experimental validation of the pyrolysis time", *Energy Conversion and Management* vol. 144 pp. 235-242, 2017.  
[15] A. Morato-Godino, S. Sánchez-Delgado, N. García-Hernando, A. Soria-Verdugo, "Pyrolysis of *Cynara cardunculus* L. samples – Effect of operating conditions and bed stage on the evolution of the conversion", *Chemical Engineering Journal* vol. 351, pp. 371-381, 2018.  
[16] D. Geldart, "Types of gas fluidization", *Powder Technology* vol. 7 pp. 285-292, 1973.  
[17] D. Kunii, O. Levenspiel, "Fluidization Engineering", 2<sup>nd</sup> edition, Butterworth-Heinemann, Boston, 1991.  
[18] P.C. Carman, "Fluid flow through granular beds", *Transactions of the Institute of Chemical Engineers* vol. 15 pp. 150-166, 1937.  
[19] J. Sánchez-Prieto, A. Soria-Verdugo, J. V. Briongos, D. Santana, "The effect of temperature on the distributor design in bubbling fluidized beds", *Powder Technology* vol. 261 pp. 176-184, 2014.